Optical Fiber Technology 73 (2022) 103063

Contents lists available at ScienceDirect

Optical Fiber Technology

journal homepage: www.elsevier.com/locate/yofte

Regular Articles

Metal coating enhancement of optical fiber distributed radiation sensors based on optical frequency domain reflectometry technology

Tianyuan Qiu [a], Changran Geng [a,b,*], Renyao Wu [a], Xiaobin Tang [a,b,*]

[a] Department of Nuclear Science and Technology, Nanjing University of Aeronautics and Astronautics, Nanjing 210016, People's Republic of China
[b] Key Laboratory of Nuclear Technology Application and Radiation Protection in Astronautics, Ministry of Industry and Information Technology, Nanjing 210016, People's Republic of China

ARTICLE INFO

Keywords:
Metal fiber coating
Fiber RIA effects
Monte Carlo simulation toolkit
OFDR

ABSTRACT

This study aimed to investigate the use of metal coatings for enhancing the radiation sensitivity of optical fibers. Monte Carlo simulations were conducted for a preliminary study of the enhancement effects of different metals and thicknesses on radiation sensitivity. The enhancement effect on radiation sensitivity was further verified by through an accelerator irradiation experiment. In this study, optical frequency domain reflectometry (OFDR) technology was used to determine changes in the radiation sensitivity of the optical fibers. The results show that the attenuation of the optical fiber with a lead metal coating was approximately-three times higher than that without a coating. Acceptable agreement was obtained between the simulation and experimental results. In conclusion, using lead-metal coating reduced the detection limit of the optical fiber dosimetry by 66%.

1. Introduction

Radiation dose monitoring is important for applying nuclear technology [1–3]. Dose measurement must be remote, online, and distributed [4].

Optical fiber sensors have many unique advantages, such as anti-electromagnetic interference, mechanical flexibility, small size, and light weight [5–7]. Using the optical time domain reflectometry (OTDR) interferometry [8], point sensors (such as fiber Bragg gratings [9]) and Micro optical sensors (such as silicon light-emitting devices monolithically [10]) have been used to monitor physical parameters such as temperature and strain. When optical fibers are used in radiation dose measurement, three macroscopic effects of optical fibers in the radiation field are mainly used: Radiation-induced emission (RIE), Radiation-induced refractive index change (RIRIC), and Radiation-induced attenuation (RIA). For the RIE effect, it mainly uses the Cherenkov light [11] or the scintillation photons [12] generated by the fiber. The research on RIRIC effect is mainly for the application of the fiber Bragg grating (FBG) [13] and long period gratings (LPG) [14–16]. Irradiation of FBG or LPG by photons caused wavelength shift (Bragg wavelength or resonance wavelength). The dose is obtained according to the wavelength shift.

For the RIA effect, radiation-induced point defects in optical fibers under ionizing radiation are called color centers [17]. The generation of color centers weakens the strength of the transmitted signal in the fiber [18]. Dosimetry based on RIA measurements was performed in the early 90s [19–21] and was first implemented at the accelerator in 2004 by Henschel et al. [22]. Studies have shown that in the case of P-doped fibers, the expected RIA that corresponds to a dose of 300 Gy would be approximately 1.3 dB/m at a wavelength of 1300 nm [23]. In the case of Al-doped fibers, their RIA can reach 4.8 dB/m in the linear variation range [24]. For silica core fibers undoped with related elements, studies have shown that ultra-low loss pure silica core fiber (ULL-PSC) fibers from Corning can achieve RIA levels of 2 dB/m at a dose of 2000 Gy [25].

Previous studies have focused on the doping of elements in the core to enhance the RIA effect of the optical fiber to achieve radiation dosimetry at relatively low doses [26–28]. In addition, optical time domain reflectometry (OTDR) has been employed in previous studies to obtain distributed dose measurements. However, OTDR technology has a lower spatial resolution (several meters to tens of meters) [8,29]. Optical frequency-domain reflectometry (OFDR) has also been proposed to achieve higher-resolution radiation dose measurements [30]. OFDR is a reflectometer system used for measuring distributed fiber-optic backscatter with micron-scale spatial resolution [31], with high

* Corresponding authors at: Department of Nuclear Science and Technology, Nanjing University of Aeronautics and Astronautics, Nanjing 210016, People's Republic of China.
E-mail addresses: gengchr@nuaa.edu.cn (C. Geng), tangxiaobin@nuaa.edu.cn (X. Tang).

https://doi.org/10.1016/j.yofte.2022.103063
Received 12 August 2022; Received in revised form 12 September 2022; Accepted 14 September 2022

signal-to-noise ratio, high spatial resolution, and high sensitivity in the field of optical fiber sensing.

A metal coating was used in this study to increase the RIA To further improve the sensitivity of distributed dose measurement. The Monte Carlo Geant4 toolkit was used to simulate the influence of a metal layer on dose deposition in the fiber core. In addition, the effect of the actual improvement of the metal layer on the optical fiber radiation sensitivity was verified through an experiment with an accelerator irradiating the optical fiber.

2. Materials and methods

In this study, Monte Carlo tool kit Geant4 was used to simulate the deposition dose in the optical fiber core to obtain the best parameters. According to the simulation results, the corresponding metal layer and thickness are selected to carry out the actual optical fiber irradiation experiment. The setup of simulation and experiment were introduced in this section.

2.1. *Configurations of the Monte Carlo simulation*

This section includes physical lists, radioactive sources, and geometric models used in GEANT4 simulations.

2.1.1. *Physics list and source definition in the simulation*

Geant4 is a general-purpose Monte Carlo simulation toolkit for particle transportation and has been widely used in the field of nuclear technology applications [32]. In this study, the detailed transport of ionizing radiation and dose deposition were simulated using the “Standard Electromagnetic Physics” a Physical List in the Geant4 Monte Carlo Toolkit (version 10.06. p01). The optical fiber was vertically irradiated with 6 MV and 10 MV photons [33,34]. A surface source with a diameter of 4 cm was placed close to the solid water surface and emitted particles perpendicular to the fiber. All simulations were performed using 1×10^9 primary particles to maintain a statistical uncertainty below 0.5 %.

2.1.2. *Geometry structure applied in the simulation*

The Geometric structure applied in the simulation is shown in Fig. 1. Three fibers with a length of 10 cm were placed side-by-side with a spacing of 0.3 cm. The outer dimensions of the coating, cladding, and core of the optical fiber were 245, 125, and 9 μm, respectively. The core and cladding materials were silica dioxide, and the coating was polyimide. The densities of the core and cladding were 2.2 g/cm^3, whereas the coating density was 1 g/cm^3. Since the polyimide layer does not affect the experimental results. After removing the original polyimide coating, the fiber becomes so fragile that experiments are difficult to perform. Therefore, we keep the original coating layer for experiment and simulation. Square metal layers with an area of 10 × 10 cm were placed above and below the optical fibers. The metal layers were used to simulate the coatings of the fibers, similar to a study conducted by Debnath et al. [35]. Three materials—lead, copper, and aluminum—were used as metal layers. To ensure a charged particle equilibrium in the fiber, layers of solid water with different thicknesses, depending on the photon energy, were placed on the outer side of the metal layer: a thickness of 1.5 cm was used for 6 MV photons and a thickness of 2 cm was used for 10 MV photons.

2.2. *Experimental procedure*

Based on the Geant4 simulation, the radiation sensitivity enhancement of the metal-coated fiber was verified through an accelerator (Varian TrueBeam) irradiation experiment. The transmission spectra of the silica-core fiber (SMF-28) and radiation-sensitive fiber (IXF-RAD-SENSE-SM-1550-PI) [36] under irradiation were measured before the experiment. An appropriate optical fiber was selected for follow-up experiments based on the spectral change characteristics of the two optical fibers after irradiation.

In the experiment, the OFDR technology (OCI-T Wuhan Haoheng) was used to measure the attenuation change of the optical fiber under irradiation. Multiple groups of optical fibers were connected through an FC/APC flange to simultaneously measure the signal attenuation of the optical fibers. The average value of all data within every 2 cm of the fiber, considered as the measurement point, was taken to improve the stability of the measurement results. Fiber attenuation was obtained by calculating the difference between the signals at the start and end of the region of interest.

The experimental setup is shown in Fig. 2. Since the RIA measurement results are attenuation per unit length of the optical fiber, four groups of 1-m long optical fibers were used. Lead, copper, or aluminum sheets of 0.6 mm thickness were placed above and below in each of the three groups to simulate coatings of the optical fibers. A group without a metal covering served as the control group. Solid water with a 1.5 or 3 cm thickness, depending on the photon energy used, was placed above the metal sheet to ensure charged particle equilibrium in the fiber during irradiation. The optical fiber was placed under a linear accelerator (source-to-axis distance (SAD) = 100 cm). In this experiment, 6 and 10 MV energies were used for irradiation at dose rates of 6 and 3 Gy/min, respectively. Signals were recorded every 5 Gy, and each group was irradiated with a total dose of 60 Gy. During irradiation, the size of the radiation field was controlled to 36 cm × 36 cm to ensure that all the fibers were in the radiation field. The uncertainty of the dose received by each group of fibers was less than 4 %, which was verified using an EBT3 film before the experiment.

3. Results and discussion

According to previous studies [37,38], the use of an optical fiber RIA combined with OFDR technology has the potential to achieve remote, online, and distributed dose monitoring. Therefore, this study developed a method for enhancing the radiation sensitivity of the fibers based on

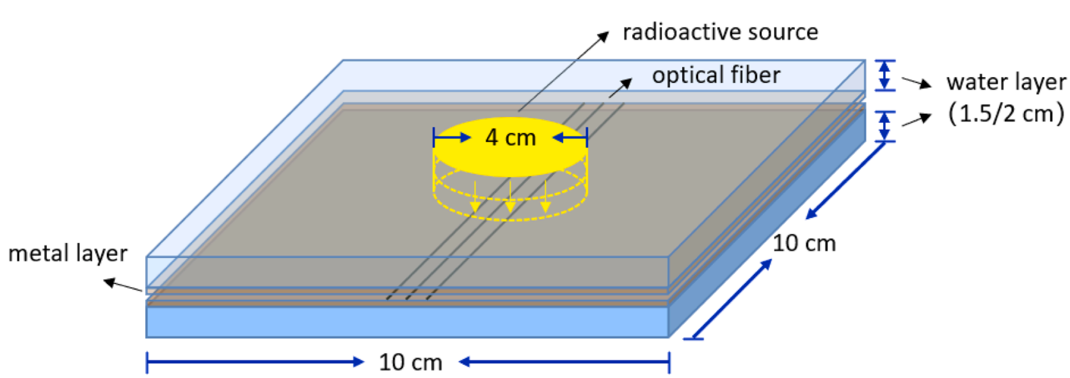

Fig. 1. Schematic of the geometry and beam setup in Geant4.

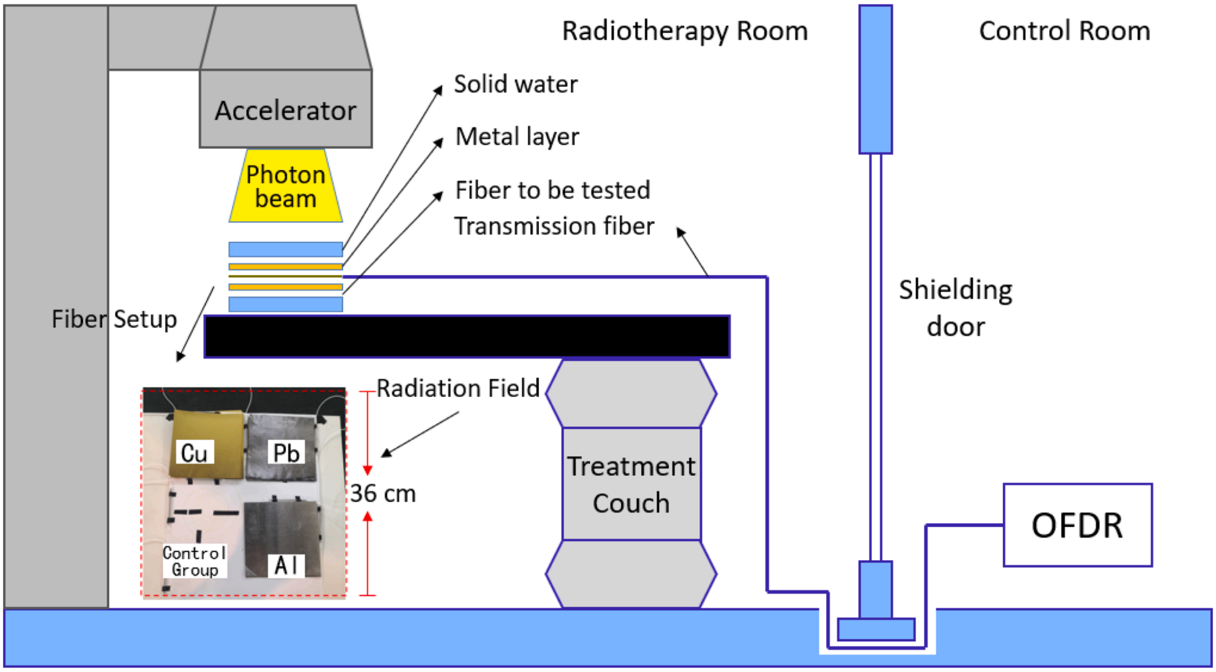

Fig. 2. Experimental setup.

fiber coating to enable better application of the fiber dosimeter in low-dose radiation environments.

3.1. *Transmission spectra of two optical fibers under irradiation*

Fig. 3 shows the near-infrared transmission RIA spectra of the SMF-28 silica and radiation-sensitive fibers. The spectra were measured using an all-band broadband light source and spectrometer under cobalt-60 irradiation. Fig. 3 shows the attenuation results of the transmission spectra of the optical fibers at a dose rate of 420 Gy/h. Based on the RIA spectrum of the SMF-28 fiber, the attenuation of the fiber did not increase significantly with irradiation time, and no obvious absorption band was observed in the 1550 nm band. In contrast, the spectrum of the IXF-RAD-SENSE-SM-1550-PI fiber exhibited an obvious absorption band near the 1550 nm wavelength, and the attenuation of the fiber changed significantly with increasing irradiation time. Considering that the center wavelength of the swept-frequency laser in the OFDR used in this experiment was 1550 nm, the RIA changes in the 1550 nm band would be useful for OFDR. The absorption band is mainly caused by IR-absorbing P1 defects [39]. Therefore, the IXF-RAD-SENSE-SM-1550-PI fiber was selected for further study.

3.2. *Simulation results*

3.2.1. *Enhancement of dose deposition in the fiber core with metal coatings subjected to 6 MV photon irradiation*

Fig. 4 shows the simulated relative dose deposition ratio for the fiber core irradiated with 6 MV accelerator photons. The relative dose ratio represents the results normalized to the dose deposition in the fiber core without a metal layer covering. The results show that the enhancement effect of dose deposition in the fiber core was substantially affected by the type of metal layer. For the same thickness of the metal layer, the metal-covered fiber core with a high atomic number had a higher dose deposition. Therefore, selecting lead as a coating material for optical fibers results in higher enhancement in radiation sensitivity. The dose deposition in the fiber core increased with the increasing thickness of the metal. When the metal layer reached a certain thickness, the dose deposition enhancement reached a plateau. As shown in the results, the maximum dose increase was reached when the thickness was 0.4 mm, with 2.4 times increase in dose deposition. In contrast, when copper and

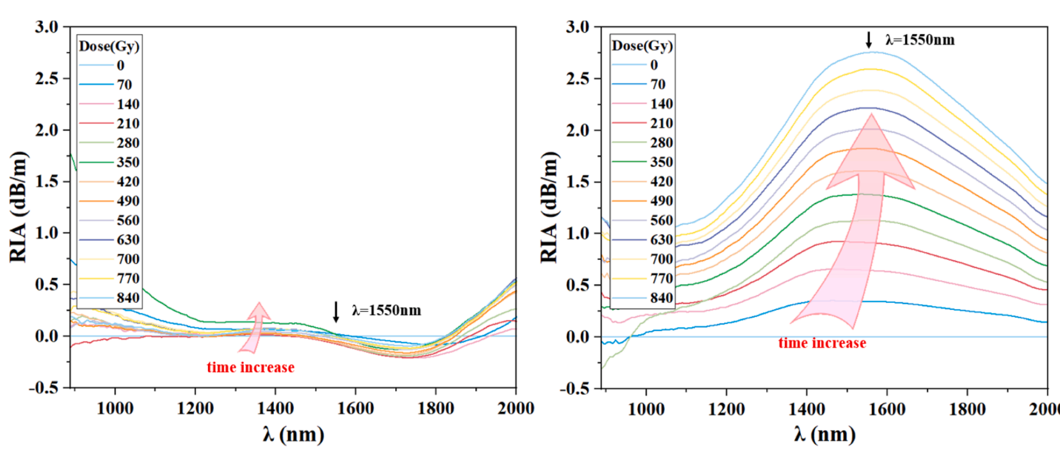

Fig. 3. Fiber RIA spectra: (a) SMF-28 fiber and (b) radiation-sensitive fiber.

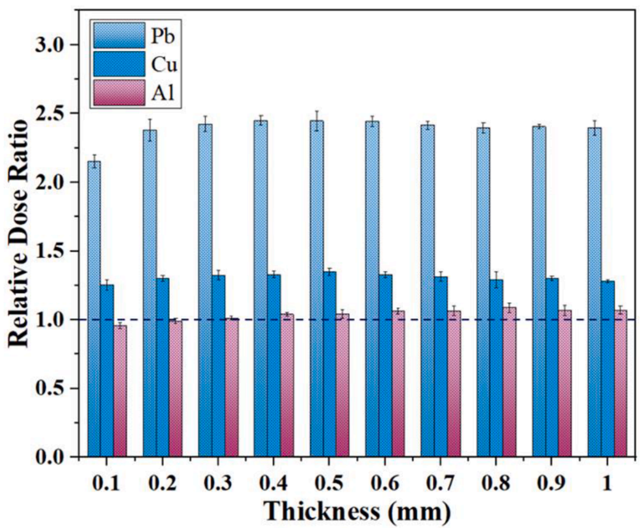

Fig. 4. Relative dose ratio at 6 MV photon irradiation.

aluminum were used, the dose deposition in the fiber core increased slowly with increasing thickness. Moreover, the increases in dose deposition by using copper and aluminum were lesser than that by using lead.

The simulation results show that using metal materials with high atomic numbers can significantly increase dose deposition in the fiber core because high-energy photons generate a large amount of secondary particles in high-Z metallic materials. Secondary particles deposit more energy in the fiber below the metal layer. Thus, the deposition dose in the fiber core increased with the thickness of the metal layer. When the metal layer reached a certain thickness, the generation and attenuation of secondary particles in the metal layer gradually reached a balance. Thus, the enhancement effect on the dose deposition tended to be stable.

3.2.2. *Enhancement of dose deposition in the fiber core with metal coatings at 10 MV photon irradiation*

Fig. 5 shows the simulation results obtained using 10 MV photons. A similar trend was observed for the 6 MV photon irradiation. A metal layer with a higher atomic number resulted in a higher dose deposition enhancement in the fiber core. A plateau for enhancement existed when a certain thickness was achieved. For 10 MV photons, when the lead plate was used, the enhancement effect reached a plateau when the thickness reached 0.6 mm, and its relative dose deposition in the fiber core was increased by 2.6 times.

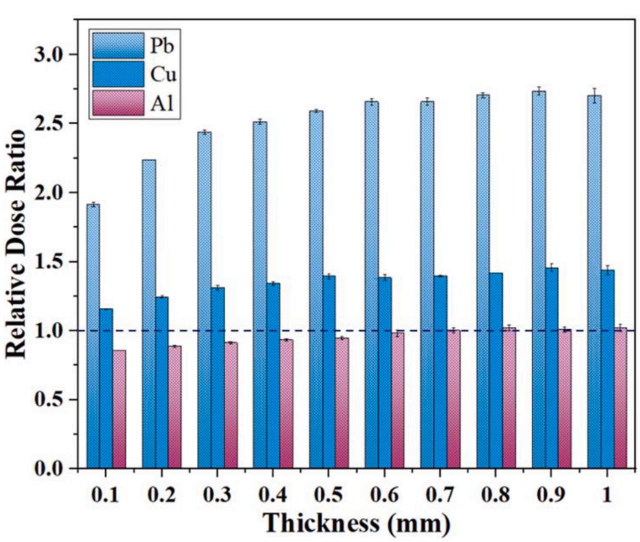

Fig. 5. Relative dose ratio at 10 MV photon irradiation.

When irradiated with photons of 10 MV energy compared to 6 MV photons, the thickness required to reach equilibrium also increased because of the increase in the primary photon energy. Therefore, in the simulation results, the use of 10 MV photons required a metal layer thickness greater than that for 6 MV photons when the dose deposition in the fiber core enhancement effect reached equilibrium.

3.3. *Experimental results*

3.3.1. *Fiber attenuation at 6 MV photon irradiation with a dose rate of 6 Gy/min*

Fig. 6 shows that the attenuation of the fiber increased with the irradiated dose. The slope of the linearly fitted curve represents the rate of change in fiber attenuation. The intercept of the fitted curve was subtracted to ensure it would start from the same position. Table 1 presents the slopes and R^2 of the fitting curves for the fibers with and without metal layers after irradiation with 6 MV photons at 6 Gy/min. The slopes of the fibers with lead, copper, and aluminum metal layers were approximately 2.52, 1.28, and 1.02 times, respectively, higher than that without a metal layer. The experimental results were consistent with the simulation results in terms of the magnitude of increase.

3.3.2. *Fiber attenuation at 10 MV photon irradiation with a dose rate of 6 Gy/min*

Fig. 7 shows the change in the fiber attenuation at 10 MV photon irradiation. Table 2 lists the slopes and R^2 of the fitted curves under this condition. Compared to 6 MV photon irradiation, higher-energy radiation caused a higher change in the attenuation enhancement of the metal coating. This result is mainly related to the fact that as the photon energy increases, the metal layer generates more secondary particles through interaction. In MOS-like device structure for the Si/SiO2 layer, similar fact observed for the silicon optical sensor [40]. Secondary particles deposit more energy, thereby increasing fiber attenuation. In the experimental results, compared with the case without a metal layer, the attenuation of the fibers with lead, copper, and aluminum metal layers increased by 3.24, 2.02, and 1.56 times, respectively.

3.3.3. *Fiber attenuation at different dose rates*

In addition to the irradiation dose and photon energy, the dose rate can also affect fiber attenuation. Fig. 8 shows the attenuation magnitudes of the fibers with and without metal layer coatings irradiated with

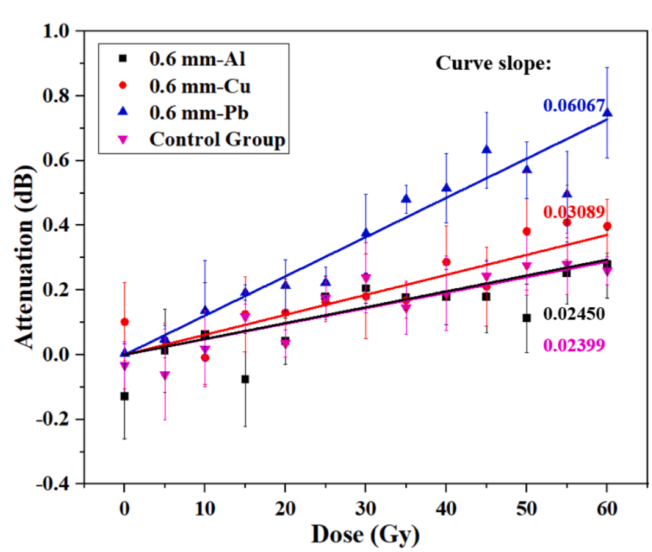

Fig. 6. Optical fiber attenuation at 6 MV photons irradiation with a dose rate of 6 Gy/min.

Table 1
Slopes of the fitting curves for the optical fibers with and without metal layers irradiated with 6 MV photons at a dose rate of 6 Gy/min.

Metal layer	Energy (MV)	Dose rate (Gy/min)	Curve slope	R^2
0.6 mm-Pb	6	6	0.06067	0.94894
0.6 mm-Cu	6	6	0.03089	0.86362
0.6 mm-Al	6	6	0.0245	0.67649
None	6	6	0.02399	0.78282

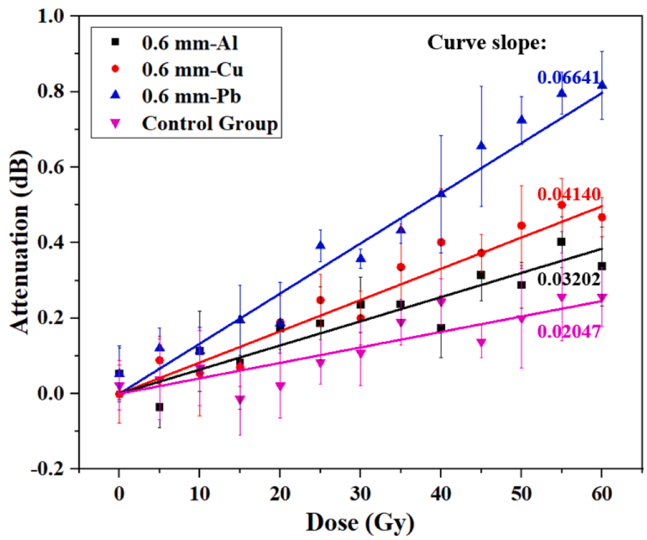

Fig. 7. Optical fiber attenuation at 10 MV photon irradiation with a dose rate of 6 Gy/min.

Table 2
Slopes of the fitting curves for the optical fibers with and without metal layers irradiated with 10 MV photons at a dose rate of 6 Gy/min.

Metal layer	Energy (MV)	Dose rate (Gy/min)	Curve slope	R^2
0.6 mm-Pb	10	6	0.06641	0.94006
0.6 mm-Cu	10	6	0.04140	0.94811
0.6 mm-Al	10	6	0.03202	0.85865
None	10	6	0.02047	0.70345

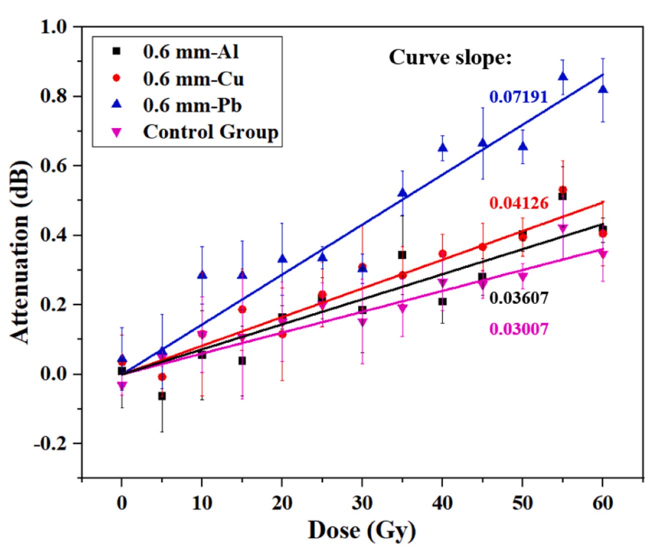

Fig. 8. Optical fiber attenuation changes at 6 MV photon irradiation with a dose rate of 3 Gy/min.

6 MV photons at a dose rate of 3 Gy/min. Table 3 lists the slopes and R^2 of the fitted curves under this condition. The slopes of the fitting curves show that compared with the case without a metal layer, the attenuation values of the fibers with lead, copper, and aluminum metal layers increased by 2.39, 1.37, and 1.19 times, respectively.

Experimental results of this study show that the largest change in fiber attenuation was obtained when the fiber was coated with a 0.6 mm lead metal layer among the studied metal layers. The optical fiber with a metal layer irradiated with 10 MV photons had higher increase in attenuation than that irradiated with 6 MV photons. At different irradiation dose rates, the results of 3 and 6 Gy/min showed no significant differences. Therefore, irradiation using two common accelerator photon irradiation dose rates, metal coating had no significant impact on the radiation sensitivity of the fiber.

3.3.4. Comparison of influencing factors

In Fig. 9, the attenuation changes slope of the optical fiber with the metal layer under the three conditions of irradiation (i.e., 6MV, 6 Gy/min; 10MV, 6 Gy/min; 6MV, 3 Gy/min) is normalized relative to the control group. The results show that the photon energy is the main influencing factor of improvement effecting under the same thickness of metal layer. The reason is that photon-silicon dioxide reaction cross-section decreases with increasing energy in the case of high energy photon. Therefore, the fiber attenuation variation is lower when the fiber without metal layer was irradiated by photons with 10MV energy. When metal layers are added, the higher energy creates more secondary electrons in the thicker metal layers. Thus metal-covered fibers have greater attenuation at higher energies. In contrast, the dose rate has no significant effect on improving effecting.

3.4. Discussion

Optical fiber radiation sensitivity is a significant problem in the application of fiber optic radiation dose sensors. In the application of distributed optic fiber sensors to radiation dose measurement, appropriate fibers need to be selected for different dose ranges. Morana et al. [36] used two types of phosphorus-doped fibers to obtain an attenuation value of 4 dB km^{-1} Gy^{-1}, and there is no rapid recovery effect of fiber after irradiation at room temperature. This phenomenon can be explained by the switching mechanism between *P*1 defects and POHCs defects related to the phosphorus element doped in the fiber. Zaghloul et al. [24] performed a distributed dose using an aluminum-doped fiber and OFDR, and an attenuation variation of 4.8 dB km^{-1} Gy^{-1} was obtained using a fitting function. Debnath et al. [35] used a metal layer in the fiber scintillator probe and obtained 1.4 times increase in the scintillation photon intensity.

Compared with previous studies, we consider for the first time to increase the RIA by adding metal coating to the fiber to improve radiation sensitivity. Monte Carlo simulation was used to simulate the influence of a metal layer on dose deposition in the fiber core. And according to the simulation results, the optimal thickness of the metal layer under different ray energies is determined. In the experiment, the metal-coated optical fiber is combined with OFDR technology to realize the online measurement of radiation dose. And the RIA changes of the metal-coated fiber under different radiation conditions are verified experimentally. Using this method can help improve the application of

Table 3
Slopes of the fitting curves of the optical fibers with and without metal layers irradiated with 6 MV photons at a dose rate of 3 Gy/min.

Metal layer	Energy (MV)	Dose rate (Gy/min)	Curve slope	R^2
0.6 mm-Pb	6	3	0.07191	0.89106
0.6 mm-Cu	6	3	0.04126	0.92775
0.6 mm-Al	6	3	0.03607	0.87473
None	6	3	0.03007	0.95418

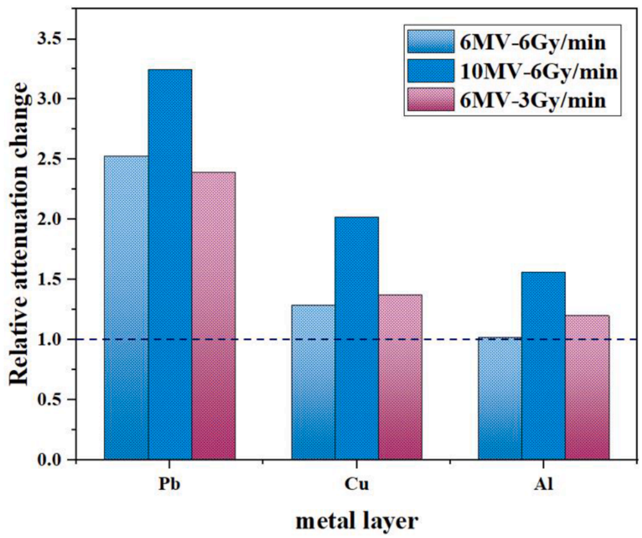

Fig. 9. Relative attenuation changes under the three conditions of irradiation: 6MV, 6 Gy/min; 10MV, 6 Gy/min; 6MV, 3 Gy/min.

optic fiber sensing technology in electronic device radiation protection and radiation dose monitoring applications.

In practical applications, the radiation dose information is reflected by the change in fiber attenuation. Therefore, its measurement range is mainly affected by the linear correspondence range between fiber attenuation and radiation dose. This range is usually determined through the formation and change in material defects during fiber irradiation. The lowest detection limit is determined by the rate of change in attenuation and detection accuracy for fiber loss. In optical fiber detection using the OFDR technology, the measurement accuracy for optical fiber attenuation is approximately ± 0.1 dB [41], which can be determined by fitting the slope of the curve in the experimental results; a dose of approximately 50 Gy was required to achieve an attenuation of 0.2 dB for a 1 m long untreated fiber. In contrast, a dose of approximately 16.6 Gy was required to achieve a 0.2 dB attenuation when the same fiber had a lead metal layer, indicating a reduction of 66 % in the minimum detection limit.

This study had some limitations. In this study, the enhancement of radiation sensitivity was investigated using a direct overlay of the metal layer. This may lead to problems with the angular response of the fiber, which is avoided by choosing vertical irradiation in this paper. Relevant metal-coated fibers will be customized for experiments in a follow-up study. In addition, the experiments in this study were performed only in a standard room-temperature environment. A follow-up study should consider the influence of environmental factors (e.g., temperature and stress) on the RIA changes of metal-coated fibers in combination with practical applications.

4. Conclusion

In this study, the enhancement of metal coating on the radiation sensitivity of optical fibers was investigated. The effect of the thickness of three metal layers on dose deposition in the core was determined. The lead metal layer exhibited the highest enhancement effect among the three studied materials. The attenuation of the fiber with a 0.6 mm lead layer coating increased by 2.52 times under 6 MV energy photon irradiation. Moreover, the attenuation of the fiber with the same metal layer increased by 3.24 times under 10 MV energy photon irradiation. No significant difference was observed in attenuation at dose rates of 3 and 6 Gy/min. The experimental results show that using optical fibers with metal layers can achieve radiation dose monitoring in low-dose radiation environments. This study helps improve the application of optical fiber sensing technology in electronic radiation protection and radiation dose monitoring applications.

CRediT authorship contribution statement

Tianyuan Qiu: Conceptualization, Methodology, Validation, Formal analysis, Investigation, Data curation, Writing – original draft, Writing – review & editing, Visualization. **Changran Geng:** Methodology, Writing – original draft, Writing – review & editing, Funding acquisition, Supervision. **Renyao Wu:** Formal analysis, Data curation, Writing – original draft, Writing – review & editing. **Xiaobin Tang:** Writing – original draft, Writing – review & editing, Funding acquisition, Supervision, Project administration.

Declaration of Competing Interest

The authors declare that they have no known competing financial interests or personal relationships that could have appeared to influence the work reported in this paper.

Data availability

Data will be made available on request.

Acknowledgments

This work was supported by the National Natural Science Foundation of China (Grant No. 12075120), Jiangsu Planned Projects for Postdoctoral Research Funds (Grant No. 2021K078A), and China Postdoctoral Science Foundation (Grant No. 2021T140321).

References

[1] V.V. Benghin, V.M. Petrov, Radiation environment monitoring for manned missions to Mars, Adv. Space Res. 31 (1) (2003) 35–38.

[2] V. Favaudon, L. Caplier, V. Monceau, F. Pouzoulet, M. Sayarath, C. Fouillade, M.-F. Poupon, I. Brito, P. Hupé, J. Bourhis, others, Ultrahigh dose-rate FLASH irradiation increases the differential response between normal and tumor tissue in mice, Sci. Transl. Med. 6 (2014) 245ra93-245ra93.

[3] A.J. Kreiner, J. Bergueiro, D. Cartelli, M. Baldo, W. Castell, J.G. Asoia, J. Padulo, J. C. Suárez Sandín, M. Igarzabal, J. Erhardt, D. Mercuri, A.A. Valda, D.M. Minsky, M. E. Debray, H.R. Somacal, M.E. Capoulat, M.S. Herrera, M.F. del Grosso, L. Gagetti, M.S. Anzorena, N. Canepa, N. Real, M. Gun, H. Tacca, Present status of accelerator-based BNCT, Reports Pract. Oncol. Radiother. 21 (2) (2016) 95–101.

[4] H. Ye, C. Geng, X. Tang, F. Tian, R. Wu, P. Xu, Radiation and temperature effect of fiber Bragg grating sensor under Co-60 irradiation, Radiat. Meas. 142 (2021), 106546.

[5] G. Eason, B. Noble, I.N. Sneddon, On certain integrals of Lipschitz-Hankel type involving products of Bessel functions, Philos. Trans. R. Soc. London. Series A, Math. Phys. Sci. 247 (1955) 529–551.

[6] A.H. Hartog, An Introduction to Distributed Optical Fibre Sensors, CRC Press, 2017.

[7] J.C. Maxwell, A Treatise on Electricity and Magnetism, Clarendon Press, 1873.

[8] I. Toccafondo, Y.E. Marin, E. Guillermain, J. Kuhnhenn, J. Mekki, M. Brugger, F. D. Pasquale, Distributed optical fiber radiation sensing in a mixed-field radiation environment at CERN, J. Lightwave Technol. 35 (16) (2017) 3303–3310.

[9] A.G. Leal-Junior, C.A. Díaz, A. Frizera, C. Marques, M.R. Ribeiro, M.J. Pontes, Simultaneous measurement of pressure and temperature with a single FBG embedded in a polymer diaphragm, Opt. Laser Technol. 112 (2019) 77–84.

[10] K. Xu, Y. Chen, T.A. Okhai, L.W. Snyman, Micro optical sensors based on avalanching silicon light-emitting devices monolithically integrated on chips, Opt. Mater. Express 9 (2019) 3985–3997.

[11] P. Xu, C. Geng, D. Shu, X. Tang, H. Liu, F. Tian, H. Ye, Two-dimensional dose distribution measurement based on rotational optical fiber array: A Monte Carlo simulation study, Radiat. Meas. 142 (2021) 106556.

[12] S. Song, J. Kim, J.H. Park, S. Kim, T. Lim, J.H. Kim, J.H. Moon, B. Lee, High-spatial-resolution position-sensitive plastic scintillation optical fiber bundle detector, in: Photonics, MDPI, 2021: p. 26.

[13] A.I. Gusarov, D.S. Starodubov, F. Berghmans, O. Deparis, Y. Defosse, A. F. Fernandez, M.C. Decreton, P. Megret, M. Blondel, Design of a radiation-hard optical fiber Bragg grating temperature sensor, in: Photonics for Space and Radiation Environments, SPIE, 1999, pp. 43–50.

[14] F. Esposito, A. Srivastava, S. Campopiano, A. Iadicicco, Radiation effects on long period fiber gratings: A review, Sensors 20 (2020) 2729.

[15] F. Esposito, A. Stancalie, C.-D. Negut, S. Campopiano, D. Sporea, A. Iadicicco, Comparative investigation of gamma radiation effects on Long Period Gratings and

optical power in different optical fibers, J. Lightwave Technol. 37 (18) (2019) 4560–4566.

[16] F. Esposito, A. Stancalie, A. Srivastava, M. Śmietana, R. Mihalcea, C. Neguț, S. Campopiano, A. Iadicicco, The impact of gamma irradiation on optical fibers identified using Long Period Gratings, J. Lightwave Technol. (2022).

[17] S. Girard, J. Kuhnhenn, A. Gusarov, B. Brichard, M. Van Uffelen, Y. Ouerdane, A. Boukenter, C. Marcandella, Radiation effects on silica-based optical fibers: Recent advances and future challenges, IEEE Trans. Nucl. Sci. 60 (3) (2013) 2015–2036.

[18] R. Taheri Ghahrizjani, M. Ameri, H. Jahanbakhsh, H. Sadeghi, E. Mohajerani, Ultra-high precision radiation dosimetry via laser bleaching the color centers in fast recovery optical fiber sensors, IEEE Sensors J. 20 (2020) 5935–5942, https://doi.org/10.1109/JSEN.2020.2974778.

[19] H. Bueker, F.W. Haesing, Fiber optic radiation sensors, in: R. Van Geen, F. Berghmans, M.C. Decreton (Eds.), Mol, Belgium, 1994: pp. 106–114. https://doi.org/10.1117/12.198629.

[20] H. Henschel, O. Kohn, H. Schmidt, J. Kirchhof, S. Unger, Radiation-induced loss of rare earth doped silica fibres, in: RADECS 97. Fourth European Conference on Radiation and Its Effects on Components and Systems (Cat. No. 97TH8294), IEEE, 1997: pp. 439–444.

[21] H. Henschel, O. Köhn, H. Schmidt, Optical fibres as radiation dosimeters, Nucl. Instrum. Methods Phys. Res., Sect. B 69 (1992) 307–314.

[22] H. Henschel, M. Körfer, J. Kuhnhenn, U. Weinand, F. Wulf, Fibre optic radiation sensor systems for particle accelerators, Nucl. Instrum. Methods Phys. Res., Sect. A 526 (3) (2004) 537–550.

[23] M. Brugger, E. Guillermain, I. Toccafondo, F. Di Pasquale, J. Kuhnhenn, First steps towards a distributed optical fiber radiation sensing system, in: B. Cugny, Z. Sodnik, N. Karafolas (Eds.), International Conference on Space Optics — ICSO 2014, SPIE, Tenerife, Canary Islands, Spain, 2017: p. 62. https://doi.org/10.1117/12.2304122.

[24] M.A.S. Zaghloul, A. Yan, R. Chen, M.-J. Li, R. Flammang, M. Heibel, K.P. Chen, High spatial resolution radiation detection using distributed fiber sensing technique, IEEE Trans. Nucl. Sci. 64 (2017) 2569–2577, https://doi.org/10.1109/TNS.2017.2735546.

[25] A. Morana, C. Campanella, J. Vidalot, V. De Michele, E. Marin, I. Reghioua, A. Boukenter, Y. Ouerdane, P. Paillet, S. Girard, Extreme radiation sensitivity of ultra-low loss pure-silica-core optical fibers at low dose levels and infrared wavelengths, Sensors 20 (2020) 7254, https://doi.org/10.3390/s20247254.

[26] J. Bahout, Y. Ouerdane, H.E. Hamzaoui, G. Bouwmans, M. Bouazaoui, A. Cassez, K. Baudelle, R. Habert, A. Morana, A. Boukenter, S. Girard, B. Capoen, others, Remote measurements of X-rays dose rate using a cerium-doped air-clad optical fiber, IEEE Trans. Nucl. Sci. 67 (7) (2020) 1658–1662.

[27] A. Faustov, A. Gusarov, P. Mégret, M. Wuilpart, A. Zhukov, S. Novikov, V. Svetukhin, A. Fotiadi, Application of phosphate doped fibers for OFDR dosimetry, Results Phys. 6 (2016) 86–87.

[28] A.V. Faustov, A. Gusarov, M. Wuilpart, A.A. Fotiadi, L.B. Liokumovich, I. O. Zolotovskiy, A.L. Tomashuk, T. de Schoutheete, P. Megret, Comparison of gamma-radiation induced attenuation in Al-doped, P-doped and Ge-doped fibres for dosimetry, IEEE Trans. Nucl. Sci. 60 (4) (2013) 2511–2517.

[29] D. Di Francesca, I. Toccafondo, G. Li Vecchi, S. Calderini, S. Girard, A. Alessi, R. Ferraro, S. Danzeca, Y. Kadi, M. Brugger, Distributed optical fiber radiation sensing in the proton synchrotron booster at CERN, IEEE Trans. Nucl. Sci. 65 (8) (2018) 1639–1644.

[30] M. Olivero, A. Mirigaldi, V. Serafini, A. Vallan, G. Perrone, W. Blanc, M. Benabdesselam, F. Mady, C. Molardi, D. Tosi, Distributed X-ray dosimetry with optical fibers by optical frequency domain interferometry, IEEE Trans. Instrum. Meas. 70 (2021) 1–9.

[31] A. Faustov, A. Gusarov, L. Liokumovich, A. Fotiadi, M. Wuilpart, P. Mégret, Comparison of simulated and experimental results for distributed radiation-induced absorption measurement using OFDR reflectometry, in: Fifth European Workshop on Optical Fibre Sensors, SPIE, 2013, pp. 583–588.

[32] J. Allison, K. Amako, J. Apostolakis, H. Araujo, P. Arce Dubois, M. Asai, G. Barrand, R. Capra, S. Chauvie, R. Chytracek, G.A.P. Cirrone, G. Cooperman, G. Cosmo, G. Cuttone, G.G. Daquino, M. Donszelmann, M. Dressel, G. Folger, F. Foppiano, J. Generowicz, V. Grichine, S. Guatelli, P. Gumplinger, A. Heikkinen, I. Hrivnacova, A. Howard, S. Incerti, V. Ivanchenko, T. Johnson, F. Jones, T. Koi, R. Kokoulin, M. Kossov, H. Kurashige, V. Lara, S. Larsson, F. Lei, O. Link, F. Longo, M. Maire, A. Mantero, B. Mascialino, I. McLaren, P. Mendez Lorenzo, K. Minamimoto, K. Murakami, P. Nieminen, L. Pandola, S. Parlati, L. Peralta, J. Perl, A. Pfeiffer, M.G. Pia, A. Ribon, P. Rodrigues, G. Russo, S. Sadilov, G. Santin, T. Sasaki, D. Smith, N. Starkov, S. Tanaka, E. Tcherniaev, B. Tome, A. Trindade, P. Truscott, L. Urban, M. Verderi, A. Walkden, J.P. Wellisch, D.C. Williams, D. Wright, H. Yoshida, others, Geant4 developments and applications, IEEE Trans. Nucl. Sci. 53 (1) (2006) 270–278.

[33] R.D. Foster, M.P. Speiser, T.D. Solberg, Commissioning and verification of the collapsed cone convolution superposition algorithm for SBRT delivery using flattening filter-free beams, J. Appl. Clin. Med. Phys. 15 (2) (2014) 39–49.

[34] B.J. Patil, S. Dhole, Studies on (i) Characterization of Bremsstrahlung spectra from high Z elements and (ii) Development of Neutron source using MeV pulsed electron beam and their applications, Med. Phys. 32 (2010), s38.

[35] S.B.C. Debnath, J. Darreon, A. Tallet, A. Goncalves, D. Tonneau, C. Fauquet, Signal amplification of fiber integrated X-ray detector and energy independence, IEEE Sens. J. 21 (17) (2021) 18793–18799.

[36] A. Morana, C. Campanella, E. Marin, G. Melin, T. Robin, G. Li Vecchi, D. Di Francesca, A. Boukenter, Y. Ouerdane, F. Mady, M. Benabdesselam, J. Mekki, N. Balcon, S. Girard, Operating temperature range of phosphorous-doped optical fiber dosimeters exploiting infrared radiation-induced attenuation, IEEE Trans. Nucl. Sci. 68 (5) (2021) 906–912.

[37] C. Sabatier, S. Rizzolo, A. Morana, T. Allanche, T. Robin, B. Cadier, P. Paillet, M. Gaillardin, O. Duhamel, C. Marcandella, D. Aubert, G. Assaillit, G. Auriel, A. Boukenter, Y. Ouerdane, L. Mescia, E. Marin, S. Girard, 6-MeV electron exposure effects on OFDR-based distributed fiber-based sensors, IEEE Trans. Nucl. Sci. 65 (8) (2018) 1598–1603.

[38] S. Rizzolo, C. Sabatier, A. Boukenter, E. Marin, Y. Ouerdane, M. Cannas, J. Perisse, J.-R. Mace, S. Bauer, S. Girard, Radiation characterization of optical frequency domain reflectometry fiber-based distributed sensors, IEEE Trans. Nucl. Sci. 63 (3) (2016) 1688–1693.

[39] D.L. Griscom, E. Friebele, K. Long, J. Fleming, Fundamental defect centers in glass: Electron spin resonance and optical absorption studies of irradiated phosphorus-doped silica glass and optical fibers, J. Appl. Phys. 54 (1983) 3743–3762.

[40] K. Xu, Silicon electro-optic micro-modulator fabricated in standard CMOS technology as components for all silicon monolithic integrated optoelectronic systems, J. Micromech. Microeng. 31 (2021) 054001.

[41] S. Rizzolo, A. Boukenter, E. Marin, M. Cannas, J. Perisse, S. Bauer, J.R. Macé, Y. Ouerdane, S. Girard, Vulnerability of OFDR-based distributed sensors to high γ-ray doses, Opt. Express 23 (2015) 18997–19009.